Kinetics and Stereochemistry in the Catalytic Hydrogenation of Acridine

Kinya Sakanishi, Masato Ohira, and Isao Mochida *
Institute of Advanced Material Study, Kyushu University 86, Kasuga, Fukuoka 816, Japan
Hiroshi Okazaki and Mahito Soeda
Nippon Steel Chemical Co., Ltd., Tobata, Kitakyushu 804, Japan

Hydrogenation of acridine (**1**) using a commercial Pd–Al_2O_3 catalyst was kinetically and stereochemically studied under variable conditions. A consecutive pathway, (**1**) ⟶ 9,10-dihydroacridine (**2**) ⟶ 1,2,3,4,4a,9,9a,10-octahydroacridine (**5**), which competes with hydrogenative isomerization of (**2**) to 1,2,3,4,5,6,7,8-octahydroacridine (**4**) *via* 1,2,3,4-tetrahydroacridine (**3**) or (**5**) was suggested from the observed product distributions over the time course of the reactions and their kinetic simulation. Thus, selectivity for the hydrogenated products is found to be controlled by either kinetics or thermodynamics according to the reaction conditions. Thermodynamic stabilities of the products are discussed based on quantum chemical (MNDO) and molecular mechanics (MM2) calculations to rationalize the reaction scheme. The stereoisomers of (**5**) and perhydroacridine (**6**) were identified and quantified by detail analyses using g.c.–i.r. and ^{13}C n.m.r. The stereoselectivity is governed by the preference in adsorption of the intermediates on the catalyst surface at a lower reaction temperature (150 °C); however, a higher temperature (250 °C) produces the thermodynamically stable products through equilibrium control.

Selective hydrogenation of multiring aromatic nitrogen compounds, such as acridine and carbazole found in the heavy distillate of coal liquid and petroleum, is one of the most important steps not only in more efficient denitrogenation processes for their upgrading, but also in producing useful intermediates for functional molecules.

The catalytic hydrodenitrogenation of acridine, as a typical model nitrogen compound, has been extensively investigated using Ni–Mo, Ni–W, Co–Mo, and Mo catalysts,[1–3] to elucidate the denitrogenation mechanism, where several hydrogenated intermediates have been identified, no selective synthesis being intended. The selective hydrogenations of acridine using noble metal and Adkins catalysts have been reported;[4–7] however, the details on the reaction pathway have not been clarified.

High efficiency for a two-stage hydrodenitrogenation process which was carried out successively at two different reaction temperatures, using commercial Ni–Mo and Co–Mo catalysts, has been reported.[8–10] Extensive hydrogenation of the aromatic rings occurs at the lower reaction temperature (350—380 °C) of the first stage and selective fission of the C–N bond follows at the higher temperature (*ca.* 420 °C) of the second stage. The selective hydrogenation of the first stage may bring novel features in hydrodenitrogenation. Selective hydrogenations of acridine into 9,10-dihydro and 1,2,3,4,4a,9,9a,10-octahydro derivatives were reported using various noble catalysts under milder conditions in another paper.[11]

In this paper, the hydrogenation of acridine on a Pd–Al_2O_3 catalyst is examined in terms of kinetic simulation, thermodynamics, and stereochemistry of hydrogenated products, since the kinetics and products were found to be influenced by the reaction conditions, especially the temperature. Reaction pathways including the stereochemistry of intermediates is discussed on the basis of the results. Thermodynamic stabilities of products were estimated with the aid of quantum chemical calculations of MNDO[12] and MM2.[13]

Experimental

Materials.—Commercially available acridine and decalin (solvent) of guaranteed grade (98 and 96% purity, respectively) were used without further purification. A commercial catalyst, Pd–Al_2O_3 powder (Pd 5 wt%), supplied by Nippon Engelhalt Co. was directly used without any pretreatment.

Hydrogenation Procedures and Product Analyses.—Acridine (2.0 g) was placed in an autoclave (50 ml) together with decalin (10 g) and Pd–Al_2O_3 (0.20—0.40 g). The autoclave was flushed with nitrogen three times and was then filled with pure hydrogen from a cylinder. The initial pressure of hydrogen was adjusted to give the prescribed pressures (20—70 atm) at the reaction temperatures. Since hydrogen consumption was limited, only a small change of pressure was detected during the reaction. After heating the reactor to the prescribed temperature (100—250 °C), which was maintained within ±2 °C, magnetic stirring was started. After the prescribed time, the reactor was cooled with a fan and the mixture (liquid and solid) was recovered by washing out with tetrahydrofuran. The catalyst was filtered and the liquid product including the solvent was analysed by a gas chromatograph (column SE-30; 2 m; heating rate 10 °C min^{-1} from 100 to 225 °C). Reactions were repeated three times to ascertain reproducibility. The product distribution was reproducible within 5%.

Hydrogenation of 9,10-dihydroacridine (*ca.* 80%) prepared from acridine (150 °C, 70 atm; 10 min) was performed in a similar manner under variable conditions.

The stereoisomers of 1,2,3,4,4a,9,9a,10-octahydroacridine (**5**) and perhydroacridine (**6**)[14] were identified by g.c.–i.r. and ^{13}C n.m.r.[15,16] after being isolated by fractional distillation. ^{13}C Chemical shifts of *cis,trans*-(**5**) and *trans,syn,cis* and *trans,syn,trans*-(**6**) are summarized together with ^1H n.m.r. and g.c.–i.r. spectra data in Table 1 for their identification.

Computer Simulation.—Based on product analyses during the time course of the reactions under four different conditions (combinations of temperature and pressure levels), the kinetic data were simulated by a computer according to the Scheme and the first-order rate equations (1)—(6) where [(**1**)—(**6**)] are

$$d[(\mathbf{1})]/dt = -k_{12}[(\mathbf{1})] \quad (1)$$

$$d[(\mathbf{2})]/dt = -(k_{23} + k_{24} + k_{25} + k_{26})[(\mathbf{2})] + k_{12}[(\mathbf{1})] \quad (2)$$

$$d[(\mathbf{3})]/dt = k_{23}[(\mathbf{2})] - (k_{34} + k_{35})[(\mathbf{3})] \quad (3)$$

Table 1. ^{13}C Chemical shifts δ of *cis*-(**5**), *trans*-(**5**), and *trans,syn,cis*-(**6**), and *trans,syn,trans*-(**6**)[a]

	δ(p.p.m.)			
Carbons	*cis*-(**5**)	*trans*-(**5**)	*trans,syn,cis*-(**6**) (**6a**)	*trans,syn,trans*-(**6**) (**6b**)
1	27.49	32.55	26.24	32.34
2	24.68	25.94	26.25	26.21
3	20.75	24.75	20.67	25.57
4	31.97	33.56	32.66	33.66
4a	50.05	56.12	55.18	62.10
5	113.24	113.68	33.79	33.66
6	126.59	126.66	25.77	25.57
7	116.40	116.95	26.72	26.21
8	129.21	129.70	32.84	32.34
8a	119.28	121.57	38.79	43.25
9	31.81	32.99	33.54	39.91
9a	34.63	37.66	37.62	43.29
10a	143.95	144.60	62.91	62.10

[a] ^1H N.m.r.; *trans*-(**5**): δ 2.51 and 2.89 (H-9ax and -9eq, $J_{ax\text{-}eq}$ 16.2 Hz), 3.50 (H-4a), 1.95 (H-9a), 3.68 (H-10), $J_{HNaxNH9a}$ 4.0, $J_{HN9eqNHN9a}$ 5.6 Hz; (**6b**): δ 1.43 (H-10); g.c.–i.r.; ν_{C-H} 2 939 and 2 862 cm^{-1} [*trans*-(**5**)]; 2 935 and 2 865 cm^{-1} [*cis*-(**5**)].

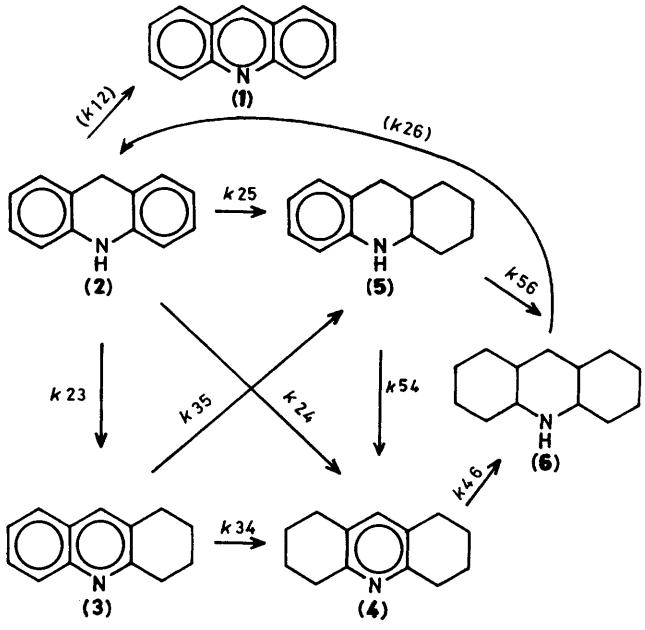

Scheme.

$$d[(4)]/dt = k_{24}[(2)] + k_{34}[(3)] + k_{54}[(5)] - k_{46}[(4)] \quad (4)$$
$$d[(5)]/dt = k_{25}[(2)] + k_{35}[(3)] - (k_{54} + k_{56})[(5)] \quad (5)$$
$$d[(6)]/dt = k_{56}[(5)] + k_{46}[(4)] + k_{26}[(2)] \quad (6)$$

the mole fractions of (**1**)—(**6**), k_{ij} are rate constants of the reaction from *i* to *j*, and k_{13} was ignored under all conditions because very little of (**3**) was found at the initial stage of the reaction under any conditions; k_{12} and k_{26} were included in the equations only when the reaction temperature and pressure were both low or both high, respectively.

Quantum Chemical Calculations of the Products.—By means of MNDO[12] for products other than perhydroacridine and MM2[13] for perhydroacridine, energetically optimized structures were determined for the respective products to enable the calculations of their heats of formation, using a FACOM M380 computer. The heats of formation of some compounds thus calculated were consistent with their observed values.

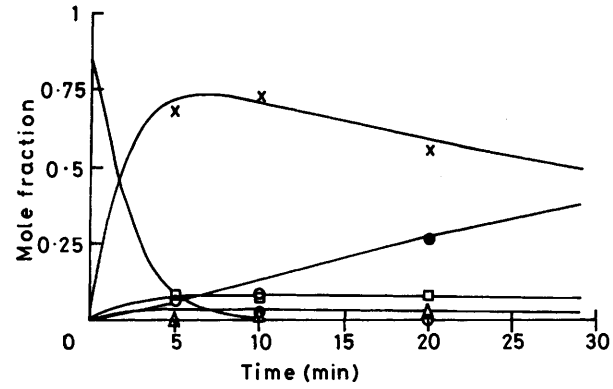

Figure 1. Hydrogenation of 9,10-dihydroacridine (**2**) at 150 °C–70 atm.: ○, (**2**); △, (**3**); □, (**4**), ×, (**5**); ●, (**6**)

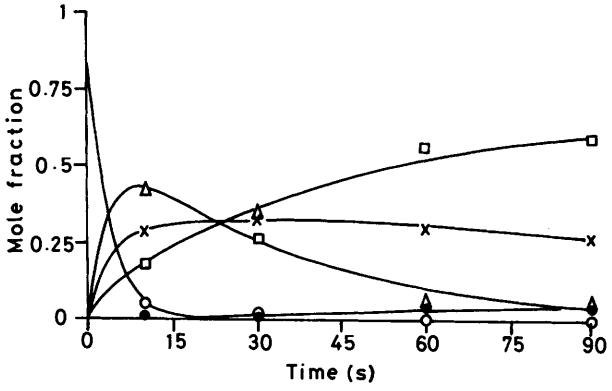

Figure 2. Hydrogenation of 9,10-dihydroacridine (**2**) at 250 °C–20 atm.: ○, (**2**); △, (**3**); □, (**4**); ×, (**5**); ●, (**6**)

Results

Kinetic Simulations.—Typical product distributions for the time course of the hydrogenation of 9,10-dihydroacridine (**2**) are illustrated in Figures 1 and 2. For low temperature–high pressure (150 °C–70 atm.) conditions, the consecutive reaction of (**1**) to (**5**) *via* (**2**) was dominant as shown in Figure 1, providing the highest selectivity for (**5**) (*ca.* 80%) with a small amount of other products after 10 min reaction time, while longer reaction times decreased its selectivity, producing (**6**).

Diverse products (**3**)—(**5**) were produced within an initial 15 s for the high temperature–low pressure (250 °C–20 atm.) conditions as shown in Figure 2. Products (**4**) became dominant after 30 s with a rapid decrease of (**3**).

Based on the product distributions in the time course of the reactions under four sets of conditions, kinetic data were simulated by a computer calculation according to the equations of (1)—(6). Some examples of fitting curves are shown in Figures 1 and 2, indicating their excellent fit with the observed points. The rate constants of each step used for fitting kinetic data under variable conditions are summarized in Table 2.

Reaction Pathways under Variable Conditions.—Hydrogenation pathways of acridine under variable conditions are illustrated in Figure 3 using the rate constants in Table 2. At 150 °C, a consecutive reaction, (**1**) ⟶ (**2**) ⟶ (**5**), is dominant regardless of hydrogen pressure. The thermodynamic deficiency

Table 2. Rate constants of the hydrogenation of acridine on $Pd-Al_2O_3$ in intermediate steps under various conditions

Reaction conditions (°C–atm.)	Rate constant (min^{-1})									
	k_{12}	k_{23}	k_{24}	k_{25}	k_{34}	k_{35}	k_{46}	k_{54}	k_{56}	k_{26}
150–20	0.02	0.005	0.018	0.12	0.01	0.005	0.001	0.04	0.001	
150–70		0.02	0.04	0.45	0.01	0.01	0.09	0.01	0.01	
250–20		10.2	1.8	4.8	1.2	0.6	0.06	0.42	0.02	
250–70		1.2	9.0	9.0	0.6	0.6	1.1	0.007	0.3	4.8

Table 3. Thermodynamic stabilities (heats of formation) of acridine and its partially hydrogenated derivatives calculated by MNDO method

	(1)	(2)	(3)	(4)	*cis*-(5)	*trans*-(5)
Heat of formation (kcal mol^{-1})	67.45	44.89	23.25	−14.65	8.23	5.01

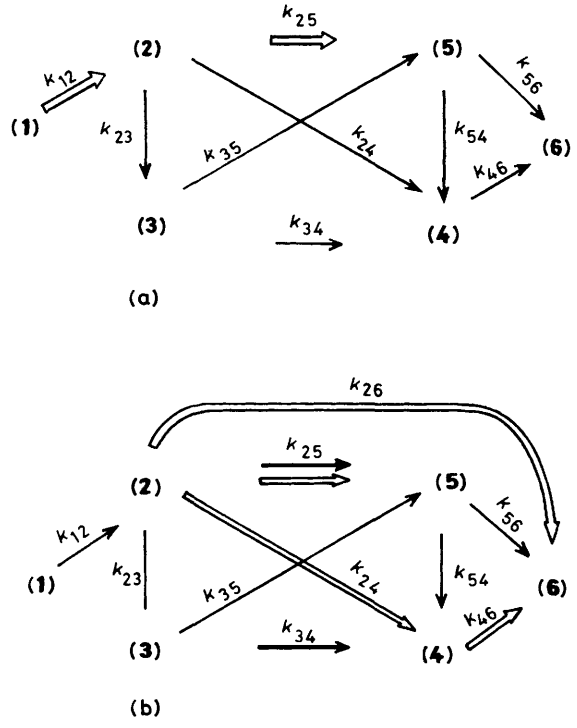

Figure 3. Reaction pathways of acridine (**1**) under variable conditions: (a) 150 °C; (b) 250 °C.→, 20 atm.; ⇨, 70 atm.

of (**5**) indicated by quantum chemical calculations (Table 3) suggests strong kinetic control at 150 °C. This lower temperature is recommended for the selective syntheses of (**2**) and (**5**) as described in a previous paper.[11]

At 250 °C, the hydrogenation pathway varied, depending on the hydrogen pressure. At 20 atm., the conversion of (**2**) into (**4**) *via* (**3**) through a hydrogenative isomerization competes with the consecutive hydrogenation of (**2**) to (**5**). The isomerization of (**2**) to (**3**) may proceed according to thermodynamic control, followed by hydrogenation to the more stable product (**4**).

In contrast, at 70 atm., the direct pathways from (**2**) to (**4**) and (**6**) were found to contribute, while the hydrogenation reactions of (**2**) to (**5**) and (**4**) to (**6**) were also very fast, leading to diverse product distributions. Such selectivities of the products at higher temperatures are determined principally by their thermodynamic stabilities as suggested by MNDO calculation.

Higher hydrogen pressure rapidly increased the rates of pure hydrogenation steps such as k_{25} and k_{56} regardless of the temperature, although the extent of increase was much higher at a higher temperature. In contrast, hydrogenative isomerization reactions such as (**2**) ⟶ (**3**), (**3**) ⟶ (**4**), and (**5**) ⟶ (**4**) tend to become slower under high hydrogen pressure, suggesting that the reaction may have dehydrogenative character.

Stereochemistry of Hydrogenation.—Both *cis*- and *trans*-isomer of (**5**) were produced at a *ca.* 2:1 ratio at 150 °C in spite of their thermodynamic stabilities as shown in Table 3, indicating that hydrogenation of (**2**) to (**5**) proceeds preferentially through *cis*-addition of hydrogen atoms. At 250 °C, the ratio of *cis*- and *trans*-(**5**) started at 2:1 in the initial 10 s and decreased to nearly unity with time.

Stereoselectivities of (**6**) in the catalytic hydrogenations of (**4**) and (**5**) (mixture of *cis*- and *trans*-isomers) on $Pd-Al_2O_3$ are summarized in Table 4. Although six configurations of the stereoisomers of (**6**) are possible according to the literature,[12] only three were found under the present conditions (Table 4). The other three isomers are thermodynamically and sterically unfavourable. The selectivities among them were very variable, depending upon the temperature in spite of definite differences in their heats of formation, steric, and σ strain energies (Table 5).

At 250 °C, *trans,syn,trans*-perhydroacridine (**6b**), whose heat of formation is smallest, was the major product regardless of the reactant [(**4**) or (**5**)] and hydrogen pressure. *trans,syn,cis* (**6a**) and *trans,anti,cis* (**6c**) isomers followed in that order. It should be noted that a significant amount of (**4**) (run 5 of Table 4) was produced from (**5**) under high temperature–low pressure conditions, indicating that a significant portion of (**6**) is produced through (**4**) thus influencing the stereochemistry of isomers (**6**).

In contrast, (**6a**) was the major product from both (**4**) and (**5**) at 150 °C in spite of having the lowest stability among three isomers (see Table 5). The selectivity for (**6a**) was much higher in the hydrogenation of (**5**) than of (**4**) as shown in Table 4. The composition of the three stereoisomers of (**6**) remained unchanged at 150 °C for longer reaction times, while (**6b**) increased at 250 °C with time.

Discussion

The reaction pathway of acridine hydrogenation varied, depending very much upon the reaction conditions. Kinetic simulations are very useful in defining the reaction pathways under variable conditions, suggesting a dominant consecutive reaction (**1**) ⟶ (**2**) ⟶ (**5**) at lower temperature and hydrogenative isomerizations (**2**) ⟶ (**3**) ⟶ (**4**) and (**2**) ⟶ (**5**) ⟶ (**4**) at higher temperature.

The selective synthesis of a particular hydrogenated product can be carried out by taking into account the temperature and pressure dependence of the rate constants of each step. Selective preparations of 9,10-dihydro-(**2**) and 1,2,3,4,4a,9,9a,10-octa-

Table 4. Catalytic hydrogenations of (4) and (5) to (6) on $Pd-Al_2O_3$

Run	Reactant	Conditions (°C–atm.–min)	Conversion (%)	Selectivity (%) (6a)	(6b)	(6c)	Other
1	(4)	250–70–30	100	15.3	80.4	3.8	0.5
2	(4)	150–70–60	100	65.9	29.2	4.0	0.9
3	(5)[a]	250–70–30	100	15.7	74.7	5.3	4.3
4	(5)[a]	150–70–60	98	93.7	0.0	1.9	4.4
5	(5)[a]	250–30–3	99	13.1	50.5	3.4	33.0[b]

[a] *cis*-(5) 64%; *trans*-(5) 28%; (4) 8%. [b] Mostly (>90%) (4).

Table 5. Thermodynamic stabilities (kcal mol^{-1}) of stereoisomers of (6) calculated by the MM2 method

	(6a)	(6b)	(6c)	(6d)	(6e)	(6f)
Heat of formation	−34.14	−42.36	−34.83	−36.24	−28.23	−25.90
Steric energy	24.74	16.52	24.05	22.64	30.65	32.98
σ Strain energy	15.20	6.92	14.50	13.10	21.11	23.44

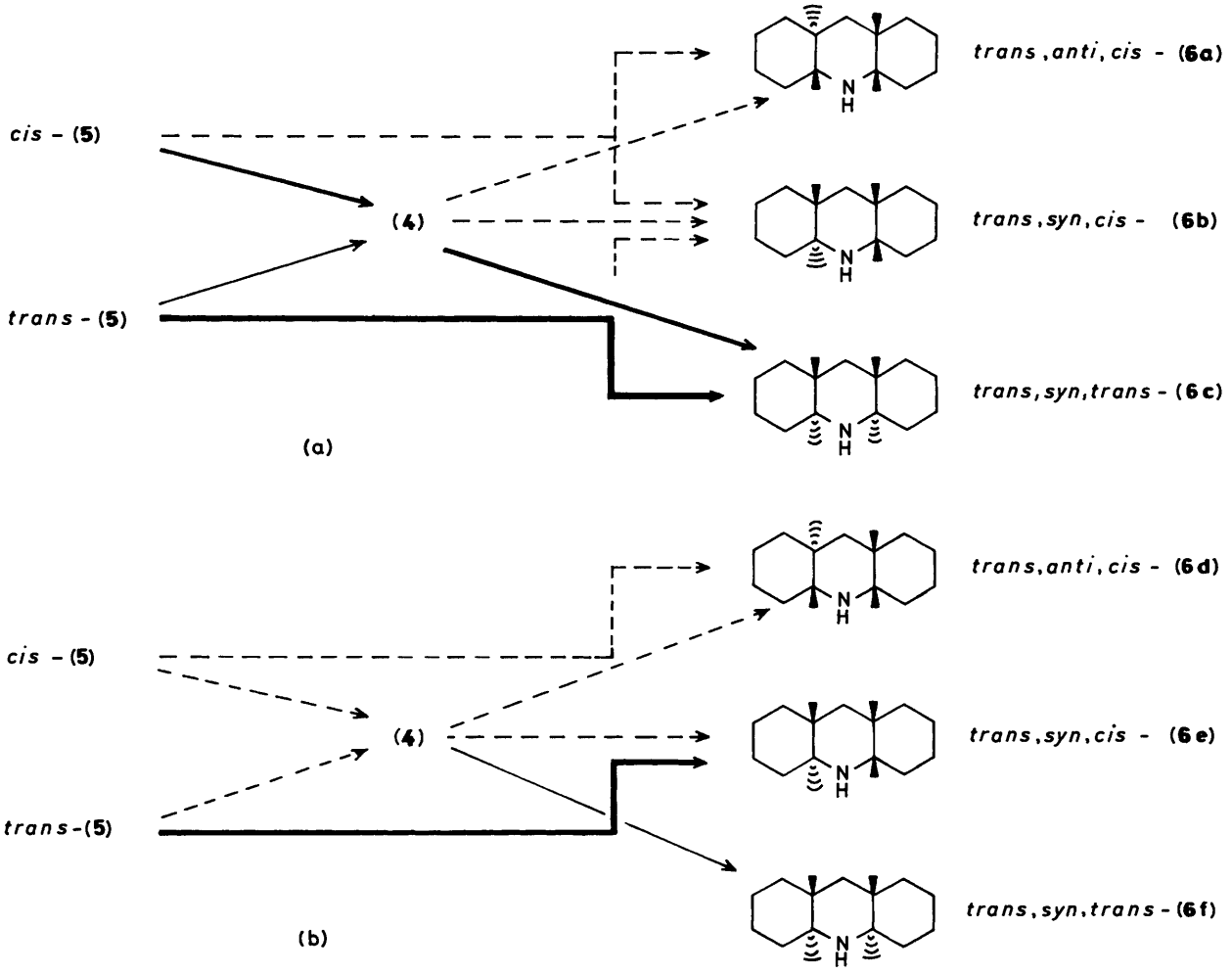

Figure 4. Reaction pathway of 1,2,3,4,4a,9,9a,10-octahydroacridine (5) to perhydroacridine (6): (a) 250 °C; (b) 150 °C

hydro-acridine (5) were achieved by controlling the reaction time for the low temperature–low or high pressure conditions, respectively, since the consecutive route (1) ⟶ (2) ⟶ (5) proceeds preferentially at the lower temperature, where the hydrogenative isomerization of (2) to 1,2,3,4,5,6,7,8-octahydro-acridine (4) is minimized.

The reactivities of the substrate and intermediates can be discussed in terms of quantum chemical reactivity indexes, thermodynamic stability, and steric hindrance to adsorption on the catalyst surface.

The 9,10-positions of acridine are most reactive to hydrogenation, giving (2), as revealed by the largest reactivity

indexes. *cis*-Addition of (**2**) to produce (**5**) is kinetically favourable on the solid surface at lower temperature, where inversion of the adsorbed species is very limited.

Hydrogenative isomerization of (**2**) to the more stable 1,2,3,4-tetrahydroacridine (**3**) competes with consecutive hydrogenation at higher temperature, since thermodynamic control becomes dominant at 250 °C, where interconversions of the intermediates become rapid through rapid dehydrogenative adsorption. Thus, the higher pressure retards the reaction, by stabilizing the hydrogenated products. Hydrogenation of (**3**) to (**4**) is very fast at the higher temperature and results in further stabilization.

Although hydrogenation of (**4**) to (**6**) at the lower temperature is supposed to proceed through *cis*-addition at the four positions 4a, 8a, 9a, and 10a, the result of *cis,syn,cis*-stereoisomer (**6e**) is sterically unstable on the catalyst surface due to the eclipsed hydrogens at C-4 and -5 as suggested by MM2 calculations, and is isomerized rapidly into (**6a** and **b**) at a *ca.* 2:1 ratio as shown in Table 4. The isomerization to the less stable (**6a**) may proceed more under the present conditions than to the more stable (**6b**). Isomer (**6e**) may be adsorbed obliquely on the catalyst surface due to the lone pair sp^3 electrons of nitrogen, preferring isomerization into (**6a**) through inversion of the single hydrogen atom at either C-4a or -10a at lower temperature.

The hydrogenation of (**4**) to (**6**) at higher temperature may proceed through the same *cis*-addition as that at lower temperature; however, it is followed by rapid isomerization through repeated hydrogen inversions to *trans,syn,trans*-stereoisomer (**6b**) of the thermodynamically most stable configuration (see Table 5), the major product at higher temperature.

The hydrogenation of (**5**) to (**6**) is influenced by steric stability in the adsorption of intermediates on the catalyst surface as well as their thermodynamic stability. The reaction pathways of (**5**) to (**6**) at lower and higher temperature are schematically illustrated in Figure 4 which is based on the results of the present study. At 250 °C, the hydrogenation of (**5**) proceeds after isomerization into (**4**), the more thermodynamic stable form, to product *trans,syn,trans*-perhydroacridine (**6b**) the most thermodynamically stable stereoisomer.

On the other hand, at 150 °C, the hydrogenation of (**5**), regardless of the starting ratio of *cis*- and *trans*-isomers, is suggested to proceed preferentially through the isomerization of *cis*-(**5**) to *trans*-(**5**), followed by *cis*-addition of the latter isomer to form *trans,syn,cis*-perhydroacridine (**6a**), since the *cis*-addition of *cis*-(**5**) forming the *cis,anti,cis* stereoisomer (**6f**) may be impossible for stereochemical reasons on the catalyst surface.

The *trans,anti,cis* stereoisomer (**6c**) is always a minor product in spite of the same level of thermodynamic stability as (**6a**). The eclipsed hydrogens located at N-10 and C-4a and -10a may sterically hinder its adsorption on the catalyst surface.

In conclusions, geometric and stereo-selectivities in the catalytic hydrogenation of acridine are controlled by both kinetic and thermodynamic factors according to the reaction conditions. Hence, the selective synthesis of a particular product can be pursued by careful selection of temperature, hydrogen pressure, and time. The preference for adsorption forms of the substrates on the solid catalyst surface may strongly influence their reactivities. Thus, the kinds of metal and support for the catalyst have a strong influence. Comparisons of noble metals (Pd, Pt, Ru, and Rh) and supports (alumina and carbon) in the design of catalysts will be reported later.

Acknowledgements

We are grateful to Nippon Steel Chemical Co. Ltd., for their analytical support with the identifications of the stereoisomers by purification, ^{13}C n.m.r. and g.c.–i.r. measurements.

References

1 S. Shih, E. Reiff, R. Zawadzki, and J. R. Katzer, *Prep. ACS Div. Fuel Chem.*, 1978, **23**, 99.
2 H. Schulz, M. Schon, D. V. Do, V. H. Nguyen, A. El-Fayoumi, and N. M. Rahman, International Conference Coal Science, Sydney, 1985, p. 114.
3 M. Nagai, K. Sawahiraki, and T. Kabe, *Nippon Kagaku Kaishi*, 1979, 1350.
4 H. Adkins and H. L. Coonradt, *J. Am. Chem. Soc.*, 1941, **63**, 1563.
5 S. Friedman, M. L. Kaufman, and I. Wender, *J. Org. Chem.*, 1971, **36**, 694.
6 T. J. Lynch, M. Banah, M. McDougall, and H. D. Kaesz, *J. Mol. Catal.*, 1982, **17**, 109.
7 R. H. Fish, A. D. Thormodsen, and G. A. Cremer, *J. Am. Chem. Soc.*, 1982, **104**, 5234.
8 I. Mochida, K. Sakanishi, Y. Korai, and H. Fujitsu, *Chem. Lett.*, 1985, 909.
9 I. Mochida, K. Sakanishi, Y. Korai, and H. Fujitsu, *Fuel*, 1986, **65**, 633.
10 I. Mochida, K. Sakanishi, Y. Korai, and H. Fujitsu, *Fuel*, 1986, **65**, 1090.
11 I. Mochida, M. Ohira, K. Sakanishi, H. Fujitsu, and H. Okazaki, *Nippon Kagaku Kaishi*, 1987, 1033.
12 M. J. S. Dewar and W. Thiel, *J. Am. Chem. Soc.*, 1977, **99**, 4899.
13 N. L. Allinger, *J. Am. Chem. Soc.*, 1977, **99**, 8127.
14 T. Masamune, M. Ohno, K. Takemura, and S. Ohuchi, *Bull. Chem. Soc. Jpn.*, 1968, **41**, 2458.
15 E. L. Eliel and F. W. Vierhapper, *J. Org. Chem.*, 1976, **41**, 199.
16 R. P. Thummel and D. K. Kohli, *J. Org. Chem.*, 1977, **42**, 2742.

Received 21*st July* 1987; *Paper* 7/1316